



THE CFD-BASED DESIGN OF A BYPASS TUNNEL TO PROVIDE THE CROSS-FLOW USED IN THE CASE OF BLADE CASCADE AEROELASTIC STUDY

Pavel PROCHÁZKA¹, Chandra S. Prasad², Pavel ŠNÁBL³, Vladislav SKÁLA⁴

¹ Corresponding Author. Institute of Thermomechanics, The Czech Academy of Sciences, Prague, Czech Republic. Tel.: +420266053313, E-mail: prochap@it.cas.cz

² Institute of Thermomechanics, The Czech Academy of Sciences, Prague, Czech Republic, E-mail: cprasad@it.cas.cz

³ Institute of Thermomechanics, The Czech Academy of Sciences, Prague, Czech Republic, E-mail: snabl@it.cas.cz

⁴ Institute of Thermomechanics, The Czech Academy of Sciences, Prague, Czech Republic, E-mail: skala@it.cas.cz

ABSTRACT

Aeroelastic stability phenomenon is still in the center of interest for many research groups and engineers, particularly in applications involving compressor or turbine blades in various turbomachinery devices. There is a lack of experimental data which could help to validate CFD simulations. Typically, the tests are running in an aerodynamic wind tunnel providing uniform flow conditions. Obviously, there is a significant radial flow component in the real applications when lower mass flow ratio occurs. The radial component can be responsible for the stall flutter occurrence and consequently the stability loss in many cases. Current experimental setups using planar blade cascades do not adequately model this radial flow effect. This study is devoted to the design of bypass (cross) flow based on CFD calculation to create appropriate flow conditions. The presence of cross-flow affecting the tilted blade cascade performing harmonic motion driven by force excitation creates a complex 3D turbulent flow field. Advanced experimental techniques, including HW and PIV anemometry, are planned in the future to analyse flow dynamics. Additionally, the blade response will be measured to determine the aerodynamic damping parameter, providing valuable insights into aeroelastic stability in turbomachinery.

Keywords: cross-flow, turbomachinery, blade cascade, CFD, PIV, HW

NOMENCLATURE

Δp	[Pa]	pressure drop
v, U	[m/s]	velocity magnitude
λ	[-]	friction coefficient
ζ	[-]	local coefficient of resistance

l	[m]	length of the tube
D	[m]	diameter of the tube
ρ	[kg/m ³]	density
y^+	[-]	dimensionless wall distance

Subscripts and Superscripts

inlet	at the inlet of the section
outlet	at the outlet of the section
STD	standard deviation
x, y, z	Cartesian coordinate system
V1-V3	design designation

1. INTRODUCTION

Nowadays, steam turbines are very often operated in non-design conditions due to the significant share of renewable energy sources in the energy network. In such a case, a lower mass flow ratio results in a redistribution of the pressure field along the blades and the creation of a spatial flow structure with a pronounced radial component in the middle area of the blades. Due to lower mass flow ratio occurrence, the inlet velocity is too low and the relative angle of attack is changed causing the tendency to stall flutter. This phenomenon, combined with a large radial velocity component, results in the appearance of vortex structures at a location approximately 90 percent of the blade span. Another vortical structure is apparent near the blade root as presented in Fig 1.

A project dealing with the aeroelastic stability of turbine-blade cascades and the influence of 3D flow structures is being solved within the Institute of Thermomechanics. To successfully achieve the goals of this project, which will be solved mainly experimentally, it is necessary to design an aerodynamic tunnel with the test section that meets the required conditions for the non-rotating blades. The 3D flow condition is met even with the

presence of the elastic blade bodies as these blades will perform harmonic oscillation with torsional and bending modes resulting in time-varying inter-blade channel width. Nevertheless, the presence of two vortical structures (first one close to the blade root and second one behind the blade tip – see figure 1) cannot be physically modelled without creation of inlet flow with a radial flow component that can be controlled according to requirements.

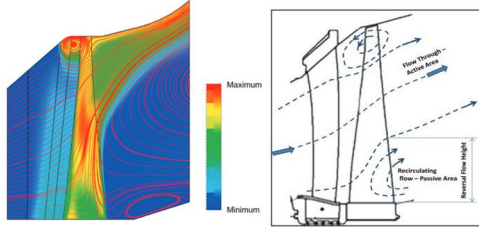


Figure 1. 3D flow structure around LP stage blade during low-load condition (Ref : [5-6])

There are several ways to introduce a radial component to channel axial flow. For example, one can utilize a fine mesh screen bended to an S-shape [1] where a shear flow is generated using the so-called Elder's generator. However, this is a passive method ensuring the desired flow parameters only in limited space behind the screen. Another passive possibility is to change the shape of the tunnel bottom and upper wall to change the flow direction or apply the test section with diverging cross section [2]. The design of such a test section adaptation is quite simple but does not offer to control the radial flow under various flow regimes. Active flow control is highly desired in this case. The air jet blowing [3] or suction effects [4] seems to be meaningful but the spatial range is not sufficient to excite the presence of the radial flow component in the entire volume of the test section. Finally, the authors have chosen the most robust solution which is not published in detail in available literature. This design was named as a bypass tunnel to create a radial velocity component across the tunnel test section. The bypass flow will be driven by a powerful ventilator which can be set independently of the main tunnel propulsion. This will allow for continuous regulation of the axial - to - radial component ratio and regulation of the size of the recirculation area.

This article will describe the calculation of desired flow rate to introduce sufficient powerful cross-flow, the calculation of pressure losses in the bypass and the choice of appropriate fan and mainly the CFD simulation of the flow in the bypass critical parts.

2. DESIGN

The aeroelastic experiments on the blade cascade will be performed inside the tunnel of Eiffel type with under pressure test section 700 x

700 mm. This tunnel has an axial motor - 14kW, 709 Pa, 44 000 m³/h (12 m³/sec), maximal airflow velocity 20-24 m/s. The model of the blade cascade will consist of 13 NACA0010 blades oriented with the stagger angle 90° and located across the test section (see figure 2). There were many numerical simulations which determined the flow rate and proper orientation of the blowing orifice (in front of the blade roots) and suction orifice (behind blade tips). The details about CFD simulation and optimization are presented in the following section. Also due to the constructional reason, it was chosen the variant with the blowing gap 650 x 100 mm located approximately 350 mm in front of the blade cascade and with one suction gap with the same cross-section (0,065 m²) which can be placed at any location on the ceiling (preferably behind the cascade). The desired flow rate was assessed as approximately 5 000 m³/h (the volume velocity 20-25 m/s). For similar flow conditions, the flow topology (figure 2) around blade cascade shows similar characteristics as required.

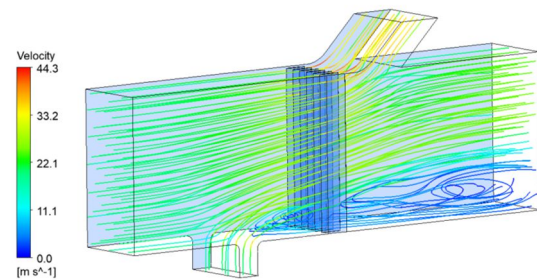


Figure 2. Flow field topology for main inlet and bypass velocity set to 20 m/s

To choose an adequate ventilator for a bypass tunnel it is crucial to know both the desired flow rate and the pressure losses due to friction and due to shaped pieces of pipeline (fittings). The main sources of resistance to flow are fluid velocity through the pipe and fluid viscosity. Pressure drop increases proportionally to the frictional shear forces within the piping network. High flow velocities or high fluid viscosities result in larger pressure losses. Low velocity will result in less pressure losses. Pressure drop is related inversely to pipe diameter to the fifth power. Pressure drop in the pipeline is directly proportional to the length of the tube. The pressure drop can be expressed as

$$\Delta p = \lambda \frac{l}{D} \frac{\rho v^2}{2} \quad (1)$$

$$\Delta p = \xi \frac{\rho v^2}{2} \quad (2)$$

for friction taking place on the inner surface of the pipes and for drop due to shape changing. The exact value of this coefficient must be determined experimentally for each fitting part.

The flow rate through the gap is $Q = 5850 \text{ m}^3/\text{h}$ for planned volume velocity 25 m/s . However, the calculation should allow for much greater velocity in case of emergency. The table 1 shows the corresponding volume velocity for different tubing cross sections and two flow rates. It is apparent that dimensions less than DN300 would result in too high velocity values and unacceptable pressure losses. The assessed pressure drop for the bypass tunnel and for velocity 30 m/s by DN300 reached the value of $3,8 \text{ kPa}$. Bigger dimension of the pipes is not practical because it involves too heavy and big parts and, more importantly, the solution is really costly.

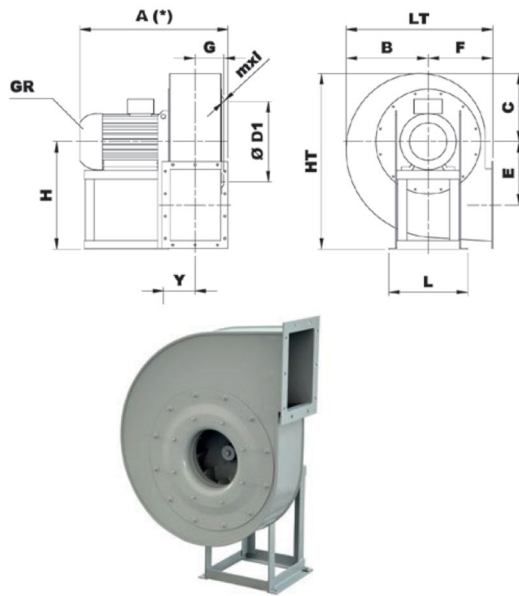


Figure 3. Radial fan ART 501N, main dimensions: outlet 322 x 229mm, inlet Ø 310mm

The ventilator which can deliver flow rate about $5\,000 - 7\,000 \text{ m}^3/\text{h}$ at pressure drop 4 kPa is already quite powerful. The axial fan cannot be used as the pressure drop is not sufficient. The radial fan ART 501, which is an industrial type usable for grain cleaners, air transport and strong filtering systems and cyclones, were finally selected. The operating point of this fan is $5000 \text{ m}^3/\text{h}$ at 4 kPa (see fan characteristic) but it can deliver about $15\,000 \text{ m}^3/\text{h}$ at minimal pressure drop.

Table 1. Tube dimensions and flow rates

	A [m ²]	7500 m ³ /h	15000 m ³ /h
DN200	0,03	69m/s	139m/s
DN300	0,07	30m/s	59m/s

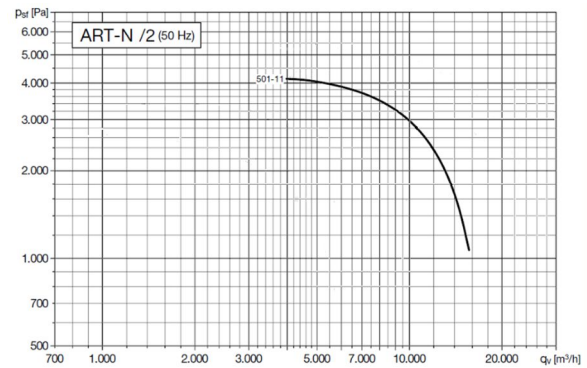


Figure 4. Radial fan performance curves, www.solerpalau.com

The pipeline of upper parts of the bypass tunnel is easy to build (figure 6 – DN300 to connect suction gap with the radial fan) as well as the tubing (322 x 229 mm) from radial fan to blowing gap. Nevertheless, there are two critical sections where the transition parts have to be applied to fit the narrow gap. The most sensitive concerning flow condition is the blowing orifice because it is preceded by one elbow. These parts of the pipeline had to be designed by CFD tools together and will be presented below.

3. CFD OPTIMIZATION

The CFD optimization was mainly used for the bypass tunnel blowing design as presented in the figure 6, to achieve 20 m/s vertical flow in front of the blade cascade. There are three design iterations that have been carried out to achieve the desired flow field.

3.1 CFD numerical model discretization

In the first step for the CFD modelling, geometry of the blowing cone is discretized using 2D and 3D FV-elements. The discretization scheme of the 1st design iteration model is presented in Fig 5.

To generate 3D FV elements first the solid wall and inlet/outlet geometry is discretized with 2D mix of rectangular/triangular elements - Fig. 5b. The fluid volume is discretized using 3D tetrahedral FV-elements - Fig. 5c. In order to capture the viscous effect accurately, 3D BL discretization is adopted. There are 7 3D BL elements used with 1st layer thickness 0.0135 mm , to obtain $y^+ < 1$, Fig. 5d. The mesh parameters are given in table 2 below.

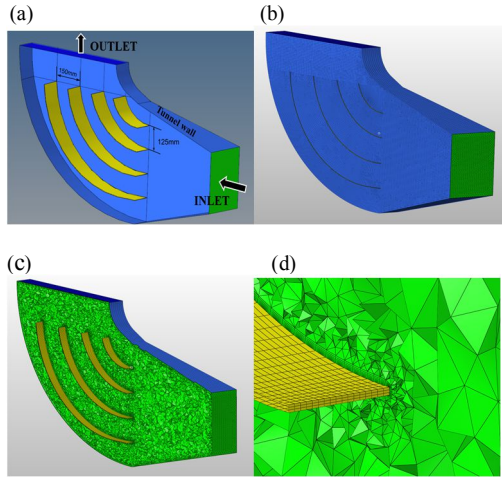


Figure 5. CFD numerical model geometry discretization using 3D FVM. (a) 1st iteration geometry (b) 2D wall surface mesh for CFD (c) interior flow field discretization using 3D tetrahedral FV-elements. (d) 3D boundary layer elements around the solid walls

Table 2. CFD numerical model discretization parameters

Mesh parameters	Value
Mesh type	FV
Average element size	7 mm
Number BL	7
Y+	< 1
First layer thickness	0.0135 mm
Mesh size	0.56 millions

Therefore, the entire fluid domain is discretized into 0.56 million FV elements. A mesh convergence study is performed prior to selecting the correct element size for discretization.

3.2 CFD numerical model

A $k-\omega$ (K- ω) SST (Shear-Stress Transport) Reynold Averaged Navier-Stokes (RANS), turbulence model is employed as CFD numerical method for the incompressible flow field simulation. Furthermore, K- ω SST turbulence model is a widely used two-equation eddy-viscosity model in computational fluid dynamics (CFD). It is designed to combine the advantages of the $k-\omega$ and $k-\epsilon$ models, providing accurate predictions in both near-wall and far-field regions [7]. The details about mathematical formulation K-

ω SST RANS model can be found in any standard CFD textbook on RANS turbulence modelling or ANSYS Fluent user manual. The 2 equation K- ω SST model is available in ANSYS Fluent 2023R1, commercial software package. All the CFD simulation for the optimization purpose is carried out in the ANSYS-Workbench 2023R1 environment.

In order to obtain the correct solution the proper boundary conditions (BC) need to be imposed in CFD models. Therefore, three main BC is imposed to correctly estimate the flow field within the blowing cone: 1) Velocity inlet type BC at INLET section of the cone - Fig 5a, 2) pressure outlet type BC at the OUTLET section - Fig 5a 3) No-slip BC are applied at the tunnel walls.

The steady state CFD simulation is carried out for all cases of optimization. The simulation time for each case approximately takes 5 hrs on 6-core AMD Ryzen 7 9800X3D processors to fully converge. Time for discretization and post processing is not included in this. However, the computational time can be reduced by using reduced order CFD methods, [8-10]. But in the present case it is not the utmost priority.

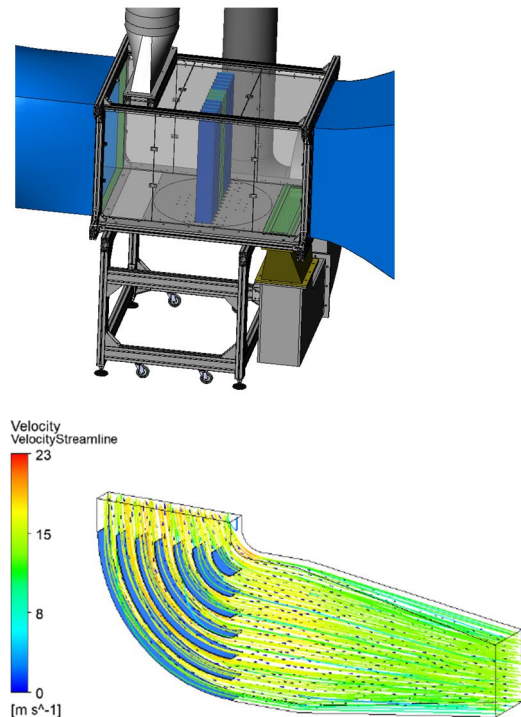


Figure 6. The design of bypass tunnel with circular pipes for suction part and an elbow and a transition part for blowing (a); CFD-optimized blowing part with several vanes to preserve the flow separation - preliminary design (b)

4. RESULTS

There were designed many variants of the pipeline to get from almost square cross-section to a very narrow rectangular shape (650 x 100 mm) while the flowing air must be turned by 90° to penetrate the main channel flow perpendicularly with perfect homogeneity. There is one of the preliminary variants in figure 6 where the change in cross-section takes place in the horizontal part, which is followed by an elbow with six guide vanes and constant cross-section. This strategy will be also applied for further variants as it is the easiest to manufacture.

There were progressively designed and CFD-verified final three variants (V1, V2 and V3) which meet the requirements also with regard to spatial possibilities. V1 is the least space-demanding as it utilizes a relatively sharp inner radius and four equidistant blades. Second and third variants are designed according to general requirements [7] utilizing four and five blades, respectively. The blade radius is 300 mm and the trailing edge is extended by 80 mm. The leading edge is shortened by 4 angular degrees. All blades are positioned proportionally with a 45° inclination. The blade thickness was set to 2 mm. The considered flow rate was set to 1.258 m³/s.

For all three variants, the design is not space-intensive and the elbow has very low pressure drop. There is a demand for outlet velocity profiles to be homogeneous along the gap width with velocity vectors only slightly deviated from the perpendicular axis. There is velocity distribution for mentioned variants inside the elbows in figure 7.

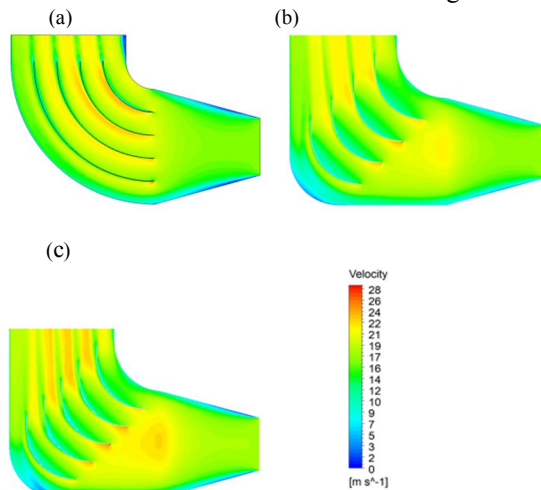


Figure 7. CFD simulation of the flow distribution inside the elbows. (a) 1st variant, (b) 2nd variant and (c) 3rd variant

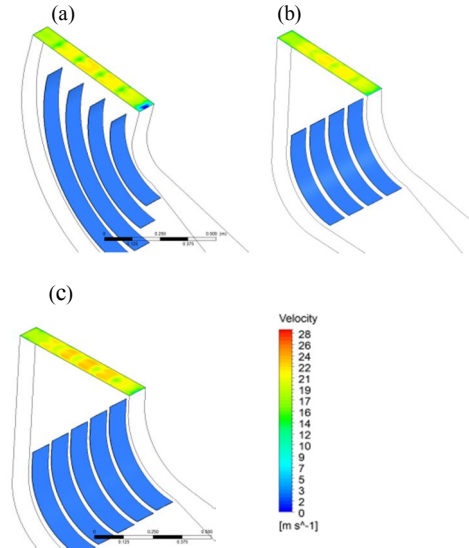


Figure 8. CFD simulation of the velocity distribution within the outlet gap. (a) 1st variant, (b) 2nd variant and (c) 3rd variant

The figure 8 is plotted to show the homogeneity of the jet to be blown. This is a crucial parameter to get a constant radial flow velocity component across the tunnel test section. It is obvious from the velocity distribution that the first variant suffers from the flow separation just behind the inner elbow radius and also the wakes behind all vanes negatively influence the smoothness of velocity distribution. Likewise, the third variant is not homogeneous along the gap. To compare more precisely, the velocity profiles at the centerline will be plotted in figure 9 for all three variants.

A solid red profile is plotted for the 1st variant. A blue dashed line and a green dash and dot line is made for variant No. 2 and 3, respectively.

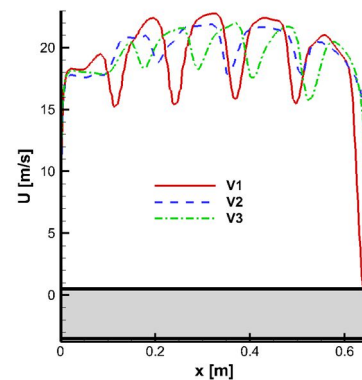


Figure 9. Velocity profiles at the outlet from the elbows V1, V2 and V3; grey area denotes the gap dimensions

All variants have an almost equivalent averaged velocity value (19.5 m/s) at the centerline. However, the velocity is not constant along this line

at all. Variant No. 1 suffers from outstanding velocity decrease inside vane wakes (peak-to-peak value 7.6 m/s). The other two variants have smaller deviations (peak-to-peak is 4.1 and 5.8 m/s for V2 and V3). A decisive indicator is the standard deviation of outlet velocity magnitude. The worst value is connected with the 1st variant where standard deviation is equal to 2.98 m/s. The third option is much better - 1.59 m/s. Second variant with only four vanes demonstrates the smallest value equal to 1.52 m/s. To specify the direction of outlet velocity vectors, the averaged angle α was evaluated based on streamwise and spanwise velocity components. The third variant has the best ratio, the second design is only slightly worse (see table 3).

Table 3. Results summary

	V1	V2	V3
STD_U [m/s]	2.98	1.52	1.59
α [°]	3.87	1.66	0.81

5. CONCLUSIONS

The bypass tunnel was designed to meet the criteria by a solution of the project dealing with 3D flow structures affecting the aeroelastic behaviour of the blade cascade with two degrees of freedom. The radial flow component will be controlled by setting of the radial fan revolutions and also by a possibility to change to position of the suction gap. While blowing jet is applied it is very crucial to design the orifice and connecting pipeline to get constant flow features along the blowing gap. This part was designed using CFD tools. Based on numerical calculations and data analysis, the second design of the elbow was selected.

Ansys Fluent proved to be very helpful in designing the partial sections of the bypass tract, which saved a lot of time when it was not necessary to tune the properties of the outlet flow. Even so, it must be taken into account that other improvements will have to apply to improve the output flow parameters.

The CFD results will be validated by the experimental measurement using hot wire (HW) anemometry. Potentially, it would be possible to add a honeycomb section and a fine mesh screen behind the elbow vanes to improve the character of the output jet.

ACKNOWLEDGEMENTS

This work was supported by the research project of the Czech Science Foundation No. 24-12144S.

REFERENCES

- [1] Antoš, P., 2014, "Development of Temperature Fluctuation in a 2D Shear Turbulent Flow", 32. *stretnutie katedier mechaniky tekutín a termomechaniky*, Conference proceeding pp. 1-4.
- [2] Uruba, V., 2012, "Stability and Dynamics of Flow in a Turbulent Boundary Layer Separation Region", *Progress in Turbulence and Wind Energy IV*, Vol. 141, pp 105-108.
- [3] Wang, J., Jiang, Ch., Zhou, X., Kang, J., Yu, S. and Bai, G., 2024, "Experimental Study on Flow Characteristics of Jet Ventilation in Crossflow in Confined Mine Spaces", *Scientific Reports*, Vol. 14, No. 8022.
- [4] He, X., Williams, D. R. and Dawson, S. T. M., 2022, "Transverse gust generation in a wind tunnel: a suction-driven approach", *Experiments in Fluids*, Vol. 63, No. 125.
- [5] Mambro, A., Congiu, F., Galloni, E. and Lanni, D., 2022. "Blade Drag Resistance in Windage Operating of Low Pressure Steam Turbines". *Fluids*, 7(12), p.372.
- [6] *Turbines, Generators and Associated Plant (Third Edition)*, Pergamon, 1991, Pages 1-123, ISBN 9780080405131.
- [7] Mehta, R. D., Bradshaw, P., "Design rules for small low speed wind tunnels", *The Aeronautical Journal of the Royal Aeronautical Society*, 1974.
- [8] Prasad, C.S. and Pešek, L., 2018. "Analysis of classical flutter in steam turbine blades using reduced order aeroelastic model", In *MATEC Web of Conferences* (Vol. 211, p. 15001). EDP Sciences.
- [9] Sepúlveda, H., Valle, R., Pincheira, G., Prasad, C.S., Salas, A., Medina, C. and Tuninetti, V., 2023. "Dynamic numerical prediction of plasticity and damage in a turbofan blade containment test", *Proceedings of the Institution of Mechanical Engineers, Part L: Journal of Materials: Design and Applications*, 237(12), pp.2551-2560.
- [10] Prasad, C.S., Šnábl, P. and Pešek, L., 2021. "A meshless method for subsonic stall flutter analysis of turbomachinery 3D blade cascade", *Bulletin of the Polish Academy of Sciences. Technical Sciences*, 69(6).